Journal of Power Sources 247 (2014) 327–331

Contents lists available at ScienceDirect

Journal of Power Sources

journal homepage: www.elsevier.com/locate/jpowsour

Short communication

Carboxymethyl chitosan: A new water soluble binder for Si anode of Li-ion batteries

Lu Yue [a, b], Lingzhi Zhang [a, *], Haoxiang Zhong [a]

[a] CAS Key Laboratory of Renewable Energy, Guangzhou Institute of Energy Conversion, Chinese Academy of Sciences, Guangzhou, Guangdong 510640, China
[b] University of Chinese Academy of Sciences, Beijing 100039, China

HIGHLIGHTS

- Carboxymethyl chitosan firstly reported as a water soluble binder for Si anode.
- Strong hydrogen bonding formed between the Si surface and carboxymethyl chitosan.
- Exhibited a high first discharge capacity of 4270 mAh g^{-1}.
- Maintained a capacity of 950 mAh g^{-1} at 500 mA g^{-1} over 50 cycles.

ARTICLE INFO

Article history:
Received 17 June 2013
Received in revised form
14 August 2013
Accepted 17 August 2013
Available online 5 September 2013

Keywords:
Nanosize Si
Carboxymethyl chitosan
Binder
Anode
Li-ion battery

ABSTRACT

Carboxymethyl chitosan (C-chitosan) is investigated as a new water soluble binder for Si anode of Li-ion batteries. The Fourier transformation infrared spectroscopy (FTIR) and X-ray photoelectron spectroscopy (XPS) measurements reveal that the strong hydrogen bonding is formed between the hydroxylated Si surface and the polar groups (−OH, −COOH and $-NH_2$) of C-chitosan. The Si/C-chitosan anode (Si:carbon black:C-chitosan = 62:30:8 in weight ratio) exhibits a high first discharge capacity (4270 mAh g^{-1}) with a first coulombic efficiency of 89%, and maintains a capacity of 950 mAh g^{-1} at the current density of 500 mA g^{-1} over 50 cycles.

1. Introduction

The major obstacle for Si anode to be used practically in Li-ion batteries is the severe volume changes during Li insertion/extraction process which consequently leads to the pulverization of the active mass particles, hence permanent capacity fade [1]. To date, three methods have been employed to overcome this problem. One is to design and prepare nanostructured Si with special morphology such as nanowire [2], nanotube [3] and nanoparticle [4]. Second is to create Si composites by dispersing Si particles in a lithium active/inactive matrix which is used as an external medium to restrain the volume change of Si [5]. The third is to screen up a suitable binder for mixing Si powder with conductive carbon additives for the preparation of Li-ion battery electrodes [6].

Polyvinylidenefluoride (PVDF) has been successfully used as the binder in commercial Li-ion batteries. However, PVDF could not give satisfying cycling stability when applied for Si anode, due to its swelling property in electrolytes and intrinsic low elasticity [7,8]. Recent studies have shown that the bio-derived water soluble polymers, such as polyacrylic acid (PAA) [9], carboxymethyl cellulose (CMC) [10] and alginate [11,12], exhibit promising perspectives as binders for Si-based anode. It was proposed that the hydrogen bonding between the carboxylic group of these polymers and Si surface is highly beneficial to reduce the damage induced by volume expansion and thus improves the cycling stability [13].

Chitin and its deacetylated derivative chitosan are natural carbohydrates-based polymers composed of randomly distributed β(1-4)-linked D-glucosamine (deacetylated unit) and N-acetyl-D-glucosamine (acetylated unit) (Fig. 1a). The abundant existence in processing discards of shrimp and crab makes them the most abundant natural polymer after cellulose. Due to the unique set of

* Corresponding author. Tel.: +86 20 37246025; fax: +86 20 37246026.
E-mail address: lzzhang@ms.giec.ac.cn (L. Zhang).

0378-7753/$ – see front matter
http://dx.doi.org/10.1016/j.jpowsour.2013.08.073

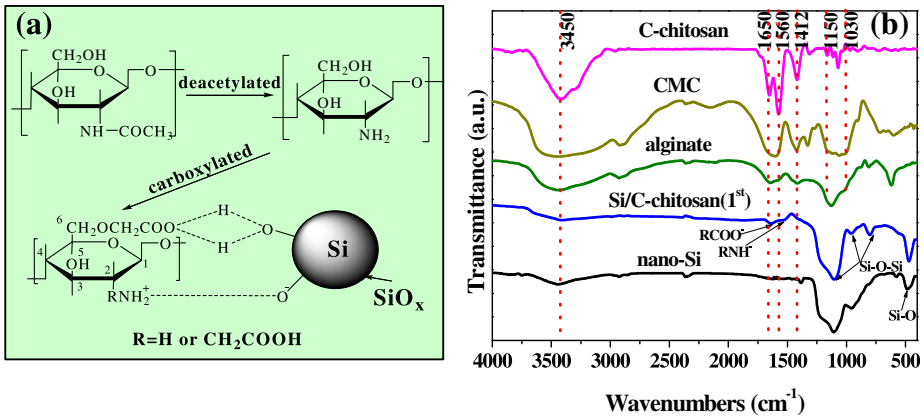

Fig. 1. (a) C-chitosan synthesis pathways and proposed C-chitosan bonding mechanism with the Si nano-particles surface; (b) FTIR spectra of C-chitosan, CMC, alginate, Si/C-chitosan (1st purified) and Si nanopowder.

useful characteristics such as biorenewabilty and biodegradability, chitin and chitosan are widely used in various fields [14]. Chitosan is a weak alkaline natural polymer which is soluble in dilute aqueous acetic acid by converting the glucosamine unit ($R-NH_2$) into its protonated form ($R-NH_2^+$). Recently, chitosan has been employed as binder in fuel cells to improve the electrochemical performance [15]. Bridel et al. has tried to use chitosan as a binder for Si anode by milling with carbon black/Si/chitosan (1/1/1 by weight ratio) in water which showed fairly moderate electrochemical performance [13].

In this communication, we report our preliminary investigation on carboxymethyl chitosan (C-chitosan), a water soluble chitosan derivative prepared by carboxymethylation of chitosan, as a new binder for Si anode, and compared with the conventional water soluble binders of CMC, alginate and the commercial non-aqueous PVDF binder was widely used in lithium-ion battery industry.

2. Experimental

Si powder with average particle sizes of 150 nm was obtained from Jiechuang New Material Technology Co. (China). PVDF (FR900, M_W = 500,000–700,000) was purchased from Dupont Co. (USA). CMC (Viscosity: 800–1200 mPaS) was purchased from Dingying Trading Co. (China). Sodium alginate (Viscosity: 1050–1150 mPaS) was obtained from Fuchen Chemicals Reagent Factory (China). C-chitosan (Viscosity: 10–80 mPaS; carboxymethylation degree ≥60%) was purchased from Aladdin Chemistry Co. (China). All materials were used as received.

To evaluate the interactions of C-chitosan with Si nanoparticles, Si powder (1 g) was dispersed in C-chitosan solution (30 ml, 3.5 wt.%, pH = 7.5) by ultrasonication for 1 h. After filtering, the Si powder was washed 4 times with DI water. The Si sample was collected in 4 portions each time after washing with DI water and dried in vacuum at 80 °C for 12 h. The firstly and fourthly collected Si sample was denoted as Si/C-chitosan (1st) and Si/C-chitosan (4th), respectively.

The coin cells (CR2025) were assembled to test the electrochemical performance. The Si powder was mixed with carbon black and binder, in a weight ratio of 62:30:8 in an aqueous solution to form homogeneous slurry. The slurry was spread onto a 10 μm thick copper foil and dried at 60 °C for 12 h in a vacuum oven and then pressed to obtain the electrode sheet with a 9–10 μm coating thickness and a loading level of about 1.4 mg cm^{-2}. The cells were assembled in an Ar filled glove-box, using 1 M $LiPF_6$ EC/DEC/DMC (1:1:1 by volume) as the electrolyte.

FTIR was recorded on a tensor 27 spectrometer (Brucker, Germany) from 4000 to 400 cm^{-1} at the resolution of 4 cm^{-1}. The XPS spectra were obtained with ESCALAB250 XPS (Thermo Fisher Scientific, USA) at 2×10^{-9} mba. Al Kα (1486.6 eV) was used as the X-ray source at 15 keV of anode voltage. The filament current and emission current were 4.6 A and 20 mA, respectively. The morphologies of the Si and composite electrodes were observed by scanning electron microscope (SEM; Hitachi S-4800, Japan) and transmission electron microscope (TEM; JEOL JEM 2100F, Japan). Electrochemical impedance spectroscopy (EIS) was measured by applying an alternating voltage of 5 mV over the frequency ranging from 10^{-2} to 10^5 Hz using a Zennium/IM6 electrochemical workstation (Zahner, Germany).

3. Results and discussion

FTIR studies were used to evaluate the interactions of C-chitosan with Si. Fig. 1b presents the FTIR spectra of C-chitosan, Si/C-chitosan (1st) and Si nanoparticles, along with that of alginate and CMC for comparison. C-chitosan exhibited several absorption peaks among 1030–1150 cm^{-1} related to saccharide structure, two peaks at 1412/1650 cm^{-1} corresponding to –COOH asymmetric/symmetric stretching vibrations, a peak at 1560 cm^{-1} related to $-NH_2$ bending vibration and a broad band at ~3450 cm^{-1} corresponding to hydrogen bonded O–H stretching vibrations [16,17]. The massive polar groups of –COOH, $-NH_2$ and –OH groups in C-chitosan would offer enough adsorption sites to generate interaction or synergistic action with Si nanoparticles [18,19]. For the Si/C-chitosan (1st), the peaks of –COOH (~1650 cm^{-1}) and $-NH_2$ (~1560 cm^{-1}) groups slightly shifted to lower wave numbers, evidencing a chemical interaction between C-chitosan and Si nanoparticles [20].

XPS measurements provided further evidence of the strong bonding between C-chitosan and Si nanoparticles. As shown in Fig. 2a, The C_{1s} XPS spectrum of the C-chitosan showed three obvious characteristic peaks corresponding to C–C and C–H bonds (284.8 eV), C–O– bond (286.4 eV) and –O–C=O bond (288.0 eV) [21,22]. In spite of careful purification by washing with water for 4 times, the Si/C-chitosan (4th) still showed strong C_{1s} and N_{1s} signal in XPS spectra (Fig. 2), indicating that a large amount of C-chitosan was still remained on the surface of Si nanoparticles. Comparing with C-chitosan, the binding energy of C–O– and –O–C=O of the water-washed Si with C-chitosan mixture increased from 286.4 to 286.6 eV and 288.0 to 288.8 eV, respectively, while the N_{1s} signal shifted from 399.9 to 399.5 eV.

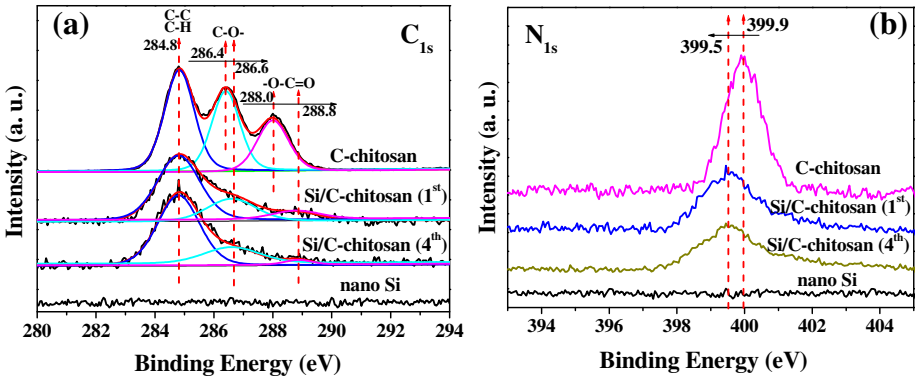

Fig. 2. XPS spectra of C_{1s} (a) and N_{1s} (b) for C-chitosan, Si/C-chitosan (1st), Si/C-chitosan (4th) and Si nanopowder.

This implied that the −OH, −COOH and $-NH_2$ groups of C-chitosan were bound to the hydroxylated Si surface and involved in the adsorption process [23,24], which was in good agreement with the FTIR analysis. These results suggested the formation of strong hydrogen bond between the hydroxylated Si surface and C-chitosan. Specially, a proposed bonding mechanism between carboxylic and amino moieties C-chitosan with the Si nanoparticle surface was given in Fig. 1a. The hydrogen bonding between the binder and Si has been previously identified as one of the most critical factors affecting the cycling performance of Si-based electrodes [11–13].

SEM studies showed that the majority of Si nanoparticles used in our work have an elliptical or spherical shape with diameter in a range of 100–200 nm and were covered with a 5–7 nm thick SiO_x layer (Fig. 3a inset). The electrode morphologies were also studied before and after 40 cycles. Before cycling, the Si

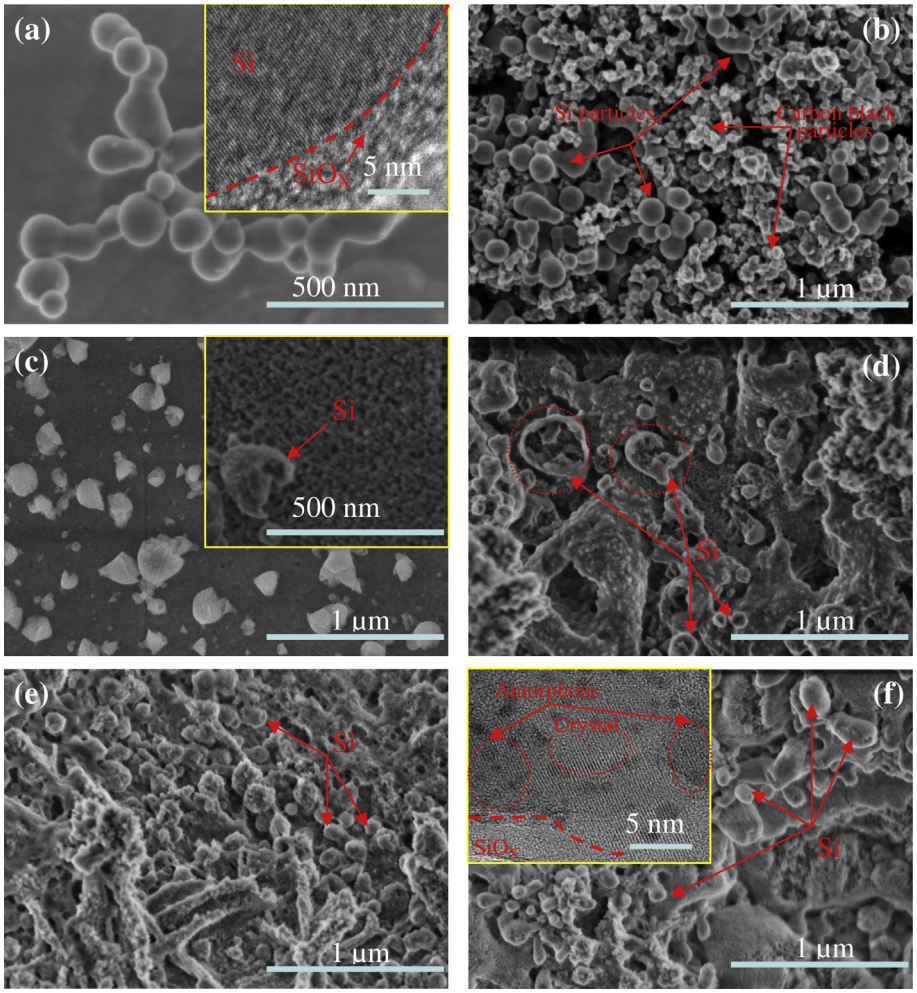

Fig. 3. SEM images of (a) Si nano-particles, (b) Si/C-chitosan/carbon black composite electrode (before cycling), and (c–f) Si anode with PVDF, CMC, alginate and C-chitosan as binder respectively (after 40 cycles) (Inset shows the corresponding transmission electron microscope (TEM) or SEM).

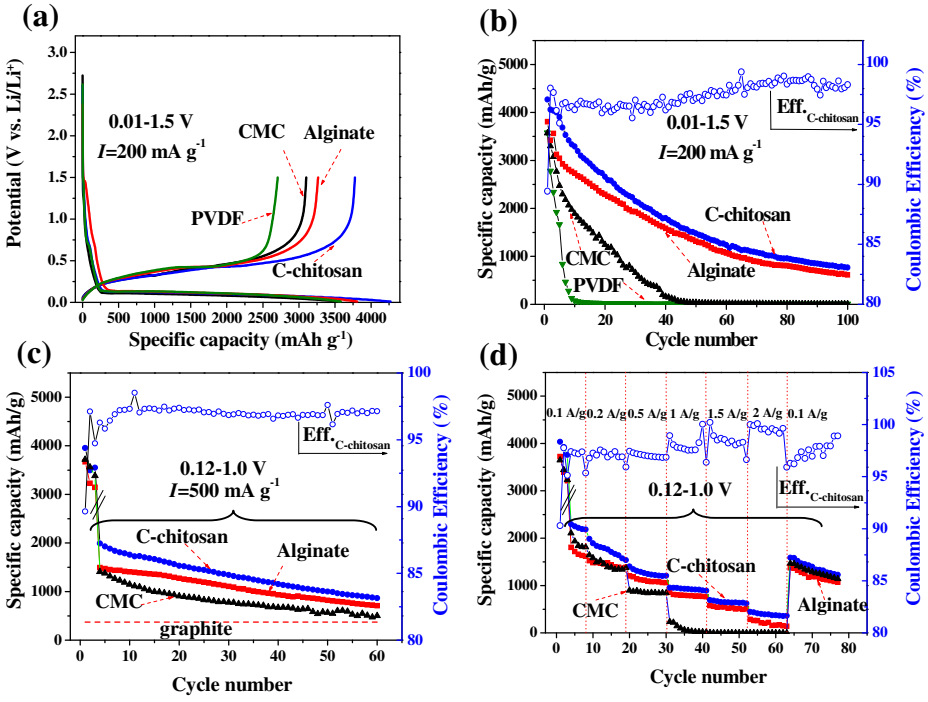

Fig. 4. (a) Comparison of first galvanostatic reduction and oxidation curves of Si anode with different binders; (b) the cycling performance of Si anode with different binders recorded at 0.01–1.5 V under 200 mA g^{-1}; (c) the cycling performance of Si anode with different binders recorded at 0.12–1.0 V under 500 mA g^{-1}; (d) rate performance of Si anode with different binders recorded at 0.12–1.0 V.

nanoparticles and smaller diameter carbon black particles (30–50 nm) were mixed homogeneously and formed a high porous texture on the electrode (Fig. 3b). After cycling for 40 times, for the Si/PVDF, only some particles were found on the surface of electrode, which could be ascribed to the escaped fractional Si from the PVDF network caused by large volume expansion over cycling (Fig. 3c). For Si/CMC, Si/alginate and Si/C-chitosan electrode, both polymeric species and Si still survived together throughout the entire electrode surface can be found (Fig. 3d–f). But there were still some broken Si nanoparticles could be found for Si/CMC compared with other two electrodes. This can be attributed to the stronger self-healing ability of latter electrodes if locally broken of Si surface during cycling [13]. For the Si/C-chitosan electrode, the cycled Si was consisted of amorphous and crystalline phases because of its transition from crystal to amorphous during the lithiation process (inset in Fig. 3f) [25].

The first galvanostatic curves were shown in Fig. 4a for the Si electrodes with different binders. All the electrodes showed an obvious charge/discharge plateau at approximately 0.4/0.2 V (vs. Li/Li^+), which was typically observed for the electrochemical lithiation of Si [1]. No other reduction and oxidation peaks from the side reactions were observed. And, the Si electrode with C-chitosan showed a higher capacity and CE of 4270 mAh g^{-1}/89% as compared with 3579 mAh g^{-1}/71%, 3589 mAh g^{-1}/87% and 3807 mAh g^{-1}/86% for the electrode with PVDF, CMC and alginate, respectively. The cycling performance of Si anode using different binders was shown in Fig. 4b. The Si/PVDF electrode showed an initial charge/discharge capacity of 2541/3579 mAh g^{-1}, then decreased quickly to almost zero. As a comparison, Si/CMC, Si/alginate and Si/C-chitosan electrodes showed the improved cycling performance. Especially, the Si/C-chitosan electrode showed an initial charge/discharge capacity

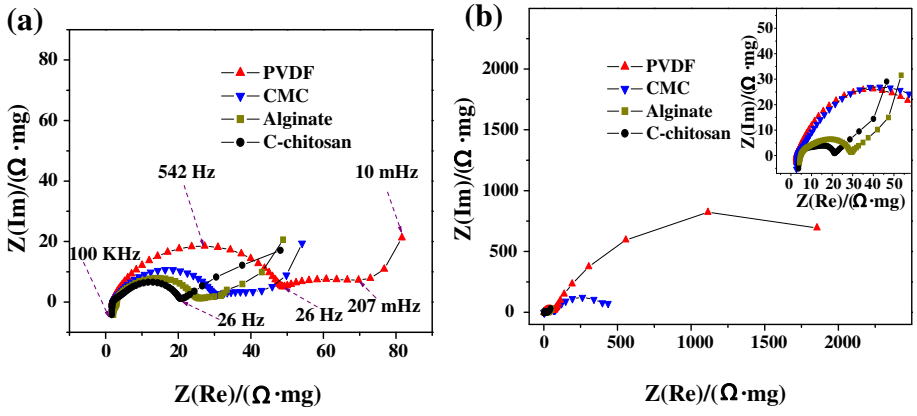

Fig. 5. Nyquist plots of Si anode with CMC, alginate, PVDF and C-chitosan as binder, respectively; (a) after 2nd cycle, (b) after 40th cycle.

of 3800/4270 mAh g^{-1} at 200 mA g^{-1}, and better cycling performance with a capacity of 1478 and 766 mAh g^{-1} at the 50th and 100th cycle respectively. To balance high capacity and cyclability [26], the electrodes with CMC, alginate and C-chitosan binder were tested between 0.01 and 1.5 V for first three cycles, then tested under a cutoff voltage of 0.12–1.0 V at 500 mA g^{-1} for the following cycles (Fig. 4c). Si/C-chitosan electrode exhibited a discharge capacity of 1990 mAh g^{-1} with a CE of 97% at the fourth cycle, and a capacity of 950 mAh g^{-1} at 50 cycles. Moreover, Si/C-chitosan cell exhibited excellent rate capabilities at the cutoff voltage (Fig. 4d). Even at a high current of 1.5 A g^{-1}, a specific capacity of 651 mAh g^{-1} was retained. When the current was changed back to 100 mA g^{-1}, the capacity quickly returned to 1588 mAh g^{-1} (72.6% of the original capacity retained). By contrast, both of the Si/alginate and Si/CMC displayed a relative worse rate performance due to their severe capacity decay with cycling.

To investigate the difference of electrochemical performance, EIS was employed to characterize the impedance properties of Si anode using different binders. Fig. 5 compared the Nyquist plots of different Si anode after 2nd and 40th cycle. For Si/PVDF and Si/CMC, both Nyquist plots were composed of a depressed semicircle in the high frequency region (26 Hz–100 KHz, reflects SEI film resistance), a semicircle in the middle frequency region (207 mHz–26 Hz, reflects the charge transfer resistance) and a sloped line in the low frequency region (10 mHz–207 mHz, reflects diffusion) [27]. For the Si/C-chitosan electrode, the middle frequency semicircle could not be observed in the Nyquist plot, probably due to the overlapping of the semicircle from SEI and the charge transfer. The Si/C-chitosan electrode showed a smaller semicircle diameter at the high and middle frequency even after 40 cycles as compared with the Si/PVDF, Si/CMC and Si/Alginate electrode, indicating an improved kinetic of electrode reactions (i.e. charge transfer and polarization). Based on the above analysis, Si/C-chitosan anode exhibited the best electrochemical characteristics and the lowest resistances, and thus the best cycling and rate performance.

4. Conclusion

We have demonstrated that C-chitosan could serve as an effective water soluble binder for Si anode of Li-ion batteries for the first time. The Si/C-chitosan anode exhibited a high first discharge capacity (4270 mAh g^{-1}) with a first CE of 89%, and better cycling and rate performance. These results open a new avenue to explore a novel series of binders from the chitosan family.

Acknowledgments

This work was supported by the National Science Foundation of China (50973112), the Hundred Talents Program of Chinese Academy of Sciences (CAS), Shenzhen Municipal Special Fund for the Development of Strategic Emerging Industries (JCYJ20120831152211489), and Guangzhou Municipal Science & Technology Project (11A44061500).

References

[1] V.A. Sethuraman, A. Nguyen, M.J. Chon, S.P.V. Nadimpalli, H. Wang, D.P. Abraham, A.F. Bower, V.B. Shenoy, P.R. Guduru, J. Electrochem. Soc. 160 (2013) A739.
[2] H. Chen, Z. Dong, Y. Fu, Y. Yang, J. Solid State Electrochem. 14 (2010) 1829.
[3] B. Chen, Q. Xu, X. Zhao, X. Zhu, M. Kong, G. Meng, Adv. Funct. Mater. 20 (2010) 3791.
[4] H. Kim, M. Seo, M.-H. Park, J. Cho, Angew. Chem. Int. Ed. 49 (2010) 2146.
[5] V. Etacheri, R. Marom, R. Elazari, G. Salitra, D. Aurbach, Energy Environ. Sci. 4 (2011) 3243.
[6] B. Koo, H. Kim, Y. Cho, K.T. Lee, N.-S. Choi, J. Cho, Angew. Chem. Int. Ed. 51 (2012) 8762.
[7] J. Li, R.B. Lewis, J.R. Dahn, Electrochem. Solid-State Lett. 10 (2007) A17.
[8] D. Munao, J.W.M. van Erven, M. Valvo, E. Garcia-Tamayo, E.M. Kelder, J. Power Sources 196 (2011) 6695.
[9] A. Magasinski, B. Zdyrko, I. Kovalenko, B. Hertzberg, R. Burtovyy, C.F. Huebner, T.F. Fuller, I. Luzinov, G. Yushin, Appl. Mater. Interfaces 2 (2010) 3004.
[10] B. Lestriez, S. Bahri, I. Sandu, L. Roue, D. Guyomard, Electrochem. Commun. 9 (2007) 2801.
[11] I. Kovalenko, B. Zdyrko, A. Magasinski, B. Hertzberg, Z. Milicev, R. Burtovyy, I. Luzinov, G. Yushin, Science 334 (2011) 75.
[12] M.-H. Ryou, J. Kim, I. Lee, S. Kim, Y.K. Jeong, S. Hong, J.H. Ryu, T.-S. Kim, J.-K. Park, H. Lee, J.W. Choi, Adv. Mater. 25 (2013) 1571.
[13] J.S. Bridel, T. Azais, M. Morcrette, J.M. Tarascon, D. Larcher, Chem. Mater. 22 (2010) 1229.
[14] F. Shahidi, J.K.V. Arachchi, Y.J. Jeon, Trends Food Sci. Technol. 10 (1999) 37.
[15] N.A. Choudhury, Y. Sahai, R.G. Buchheit, Electrochem. Commun. 13 (2011) 1.
[16] S.K. Sahu, S. Maiti, T.K. Maiti, S.K. Ghosh, P. Pramanik, J. Drug Target. 19 (2011) 104.
[17] V.K. Mourya, N.N. Inamdar, A. Tiwari, Adv. Mater. Lett. 1 (2010) 11.
[18] S. Sun, A. Wang, J. Hazard. Mater. B131 (2006) 103.
[19] M.J. Laudenslager, J.D. Schiffman, C.L. Schauer, Biomacromolecules 9 (2008) 2682.
[20] P. Liang, Y. Zhao, Q. Shen, D. Wang, D. Xu, J. Cryst. Growth 261 (2004) 571.
[21] V. Datsyuka, M. Kalyvaa, K. Papagelisb, J. Partheniosa, D. Tasisb, A. Siokoua, I. Kallitsisa, C. Galiotis, Carbon 46 (2008) 833.
[22] N. Yabuuchi, K. Shimomura, Y. Shimbe, T. Ozeki, J.-Y. Son, H. Oji, Y. Katayama, T. Miura, S. Komaba, Adv. Energy Mater. 1 (2011) 759.
[23] L. Wang, Q. Li, A. Wang, Polym. Bull. 65 (2010) 961.
[24] M. Xie, H.-H. Liu, P. Chen, Z.-L. Zhang, X.-H. Wang, Z.-X. Xie, Y.-M. Du, B.-Q. Pan, D.-W. Pang, Chem. Commun. 44 (2005) 5518.
[25] H. Kim, J. Cho, Nano Lett. 8 (2008) 3688.
[26] L. Hu, H. Wu, Y. Gao, A. Cao, H. Li, J. McDough, X. Xie, M. Zhou, Y. Cui, Adv. Energy Mater. 1 (2011) 523.
[27] D. Dees, E. Gunen, D. Abraham, A. Jansen, J. Prakash, J. Electrochem. Soc. 152 (2005) 1409.